MedChemComm

CONCISE ARTICLE

View Article Online
View Journal | View Issue

Cite this: *Med. Chem. Commun.*, 2015, **6**, 2204

Synthesis of silver nanoparticle-loaded sulfadiazine/polyvinyl alcohol nanorods and their antibacterial activities

Ping Li,[b] Xiangmin Xu,[c] Longlong Wu,[b] Binjie Li*[a] and Yanbao Zhao[b]

Received 12th August 2015,
Accepted 28th October 2015

DOI: 10.1039/c5md00331h

www.rsc.org/medchemcomm

Silver nanoparticle-loaded sulfadiazine/polyvinyl alcohol nanorods (Ag-SD/PVA NRs) were successfully synthesized in an ammonia solution, and were characterized by XRD, FT-IR, SEM and TEM. In the synthesis process, PVA was introduced to control the size of the silver sulfadiazine (SSD) precursor and further reduce SSD to produce Ag-SD/PVA NRs. The obtained Ag-SD/PVA NRs have an average width of 50 nm and a length of 300 nm, loaded with Ag NPs about 8 nm in size. As novel composite antibacterial agents, the Ag-SD/PVA NRs exhibited higher bactericidal efficacy in comparison to the Ag NPs and SSD microrods (MRs) alone. Additionally, these Ag-SD/PVA NRs showed concentration-dependent antibacterial behavior. At high concentrations, they displayed more effective antibacterial activity towards *S. aureus* than *P. aeruginosa* and *E. coli*, and at lower concentrations, they exhibited more effective antibacterial activity towards *E. coli*.

1 Introduction

Since increasing microbial infection events occur, there has been growing interest in the development of new and effective antibacterial agents.[1–4] It is well known that silver-based compounds are widely used in antibacterial materials because of their high antibacterial activity and broad antibacterial spectrum.[5,6] For example, silver sulfadiazine (SSD) is used in burn therapy. Here, silver ions provide the primary antibacterial activity against a range of bacteria and fungi, while sulfadiazine (SD) has bacteriostatic properties.[7] However, the antibacterial activity of SSD would always be discounted for its low solubility, resulting in a slow release of silver ions. Therefore, many research studies focus on improving the solubility and antibacterial efficacy of SSD by forming composite nanoparticles.[8]

Among all inorganic antibacterial agents, silver nanoparticles (Ag NPs) have been extensively studied due to their high antibacterial activity with minimal perturbation to human cells, but their practical applications are often hampered by the ease of aggregation, which would decrease their antibacterial properties. To solve this problem, different organic materials such as polymers,[9] quaternary ammonium compounds[10] and antimicrobial peptides[11] have been employed to stabilize Ag NPs and endow them with long-term synergistic antibacterial performance.

Here, we designed and fabricated novel antibacterial agents, silver nanoparticle-loaded sulfadiazine/polyvinyl alcohol nanorods (Ag-SD/PVA NRs). The nanosized SD/PVA composites possess excellent solubility in aqueous solution and provide an organic matrix to increase the stability of the Ag NPs, in which the antibacterial activities of SD and Ag NPs are combined for excellent performance of the product. To the best of our knowledge, the corresponding complex and structure haven't been reported in the literature.

2 Results and discussion

2.1 Chemistry

In a typical procedure, 0.225 g of PVA, 0.500 g of SD and 100 mL of diluted ammonia (2 wt%) were added into a flask and mixed by ultrasonic agitation to form a clear solution. Then, 2 mL of $AgNO_3$ solution (1 M) was added dropwise into the solution at room temperature with constant magnetic stirring. The colorless solution gradually changed to white, and subsequently to a light grey suspension. After reacting for 4 h, the grey precipitate was separated by centrifugation and washed with an excess amount of ethanol at least 3 times. Finally, the powder was obtained by vacuum drying at ambient temperature. As reference materials, Ag NPs and SSD microrods (MRs) were obtained *via* similar procedures but without the addition of SD and PVA, respectively.

[a] *Medical School of Henan University, Kaifeng 475004, PR China. E-mail: lbj821@163.com*
[b] *Key Laboratory for Special Functional Materials, Henan University, Kaifeng 475004, PR China*
[c] *Yellow River Conservancy Technical Institute, Kaifeng 475004, PR China*

2.2 Characterization of Ag-SD/PVA NRs

The typical XRD pattern of the Ag-SD/PVA NRs is given in Fig. 1a. In the pattern, the peaks at scattering angles 2θ of 7.1°, 11.7°, 12.8°, 14.1°, 16.5°, 19.7°, 20.9°, 21.3°, 23.8°, 26.0°, 27.4° and 28.7° are attributed to the (001), (−201), (200), (002), (011), (−210), (012), (003), (−402), (400), (212) and (004) crystal planes of monoclinic SD (JCPDS 39-1841), respectively. At the same time, the peaks at 2θ values of 17.7°, 35.9° and 37.0° are ascribed to the (002), (004) and (101) crystal planes of Ag (JCPDS 87-0598), respectively. Therefore, the sample is composed of SD and metallic silver. In addition, the peaks at 2θ values of 8.9° and 10.2° could be ascribed to the (002) and (011) crystal planes of monoclinic SSD (JCPDS 37-1555), due to the SSD precursor residue.

Fig. 1b shows the FTIR spectra of the samples. The absorption bands at 1586, 1502 and 1414 cm^{-1} are attributed to skeletal vibrations of the phenyl and pyrimidine groups of SD, respectively. Furthermore, the band at 1354 cm^{-1} belongs to the symmetrical stretching of the $-SO_2$ group, which indicates the main organic component of SD. Obviously, the band at 1430 cm^{-1} is characteristic of the O–H group deformation vibration in PVA, which indicates the presence of PVA in the composite. Additionally, the band at 1546 cm^{-1} can be assigned to the shifted ring vibration of pyrimidine due to the presence of Ag^+ ions,[12] which may be from the residue of SSD in the reduction process. In comparison, the FT-IR spectrum of SSD shows features different from that of Ag-SD/PVA. The phenyl skeletal vibration band is shifted towards a higher wavenumber from 1586 cm^{-1} to 1595 cm^{-1} and the C–C stretching vibrations of the aromatic ring are split (1595 and 1582 cm^{-1}). Therefore, it could be concluded that the organic matrix of the as-synthesized sample is mainly composed of SD instead of SSD.

The morphologies of the as-synthesized Ag-SD/PVA NRs are shown in Fig. 2. It can be seen that the sample exhibits a bundled feature with a salix leaf-like morphology (Fig. 2a). The bundles are further found to be composed of several NRs with diameters of about 50 nm and lengths of above 300 nm (Fig. 2b). To acquire more insight into the detailed microstructure of the as-synthesized sample, we conducted TEM analysis of a single nanorod separated from the bundle-like structure (Fig. 2c). It is clear that many spherical nanoparticles are homogeneously adhered to the SD NRs. Furthermore, the HRTEM image of a section of a single nanorod is shown in Fig. 2d. The lattice spacing of about 0.242 nm corresponds to the (101) crystal plane of Ag (JCPDS 87-0598). However, due the organic component of SD, there are no obvious lattice spacings in the nanorod. Additionally, the size distribution of the Ag NPs is shown in Fig. 2e. It is obvious that the Ag NPs exhibit a uniform spherical shape, and have an average size of 8 nm with a size distribution of 8 ± 2.2 nm.

The possible growth mechanism of Ag-SD/PVA NRs is illustrated in Fig. 3. Under ultrasonic conditions, hydrogen bonds between the hydroxyl groups of the PVA chains and the amine groups of the SD molecules were formed to produce SD/PVA composites. When Ag^+ ions were introduced, SSD/PVA NRs were gradually formed due to the reaction between the Ag^+ ions and SD. Meanwhile, the Ag^+ ions on the surface of the SSD/PVA NRs were reduced to Ag atoms by PVA, which led to the diffusion of the inner SSD-bound Ag^+ ions to the outer surfaces of the organic matrix and further reduction to Ag atoms.[13] Subsequently, the silver atoms were agglomerated to Ag NPs and the SSD/PVA NR precursors were gradually changed into SD/PVA NRs without a change in morphology due to the similar monoclinic structure of SSD and SD. Finally, the Ag NPs were loaded on the surface of the SD/PVA NRs through coordination bonds. In the synthesis process, PVA possesses dual functions: (a) as a reducing agent to reduce the silver ions to elemental silver and (b) as a steric hindrance agent to control the size of the SSD NRs and Ag NPs.[14]

2.3 Antimicrobial assay of Ag-SD/PVA NRs

The antimicrobial activity of Ag-SD/PVA NRs against three tested strains of *S. aureus*, *P. aeruginosa* and *E. coli* was evaluated by MIC, MBC and inhibition zone assays. For comparison, the results for the Ag NPs, SSD MRs and PVA were given. All the experiments were performed in triplicate to ensure the credibility of the data.

Minimum inhibition concentration (MIC) and minimal bactericidal concentration (MBC) methods were applied to assess the antibacterial activity of the samples.[15,16] In the MIC test, a

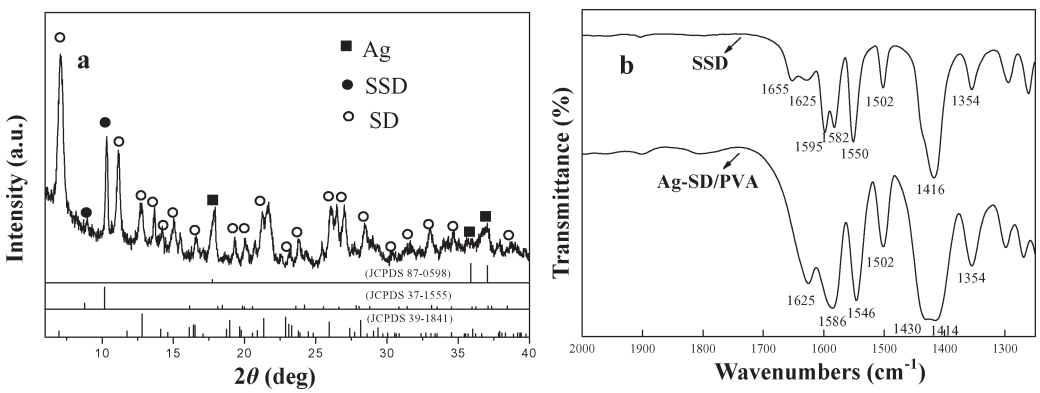

Fig. 1 (a) XRD pattern of Ag-SD/PVA NRs; (b) FTIR spectra of Ag-SD/PVA NRs and SSD MRs.

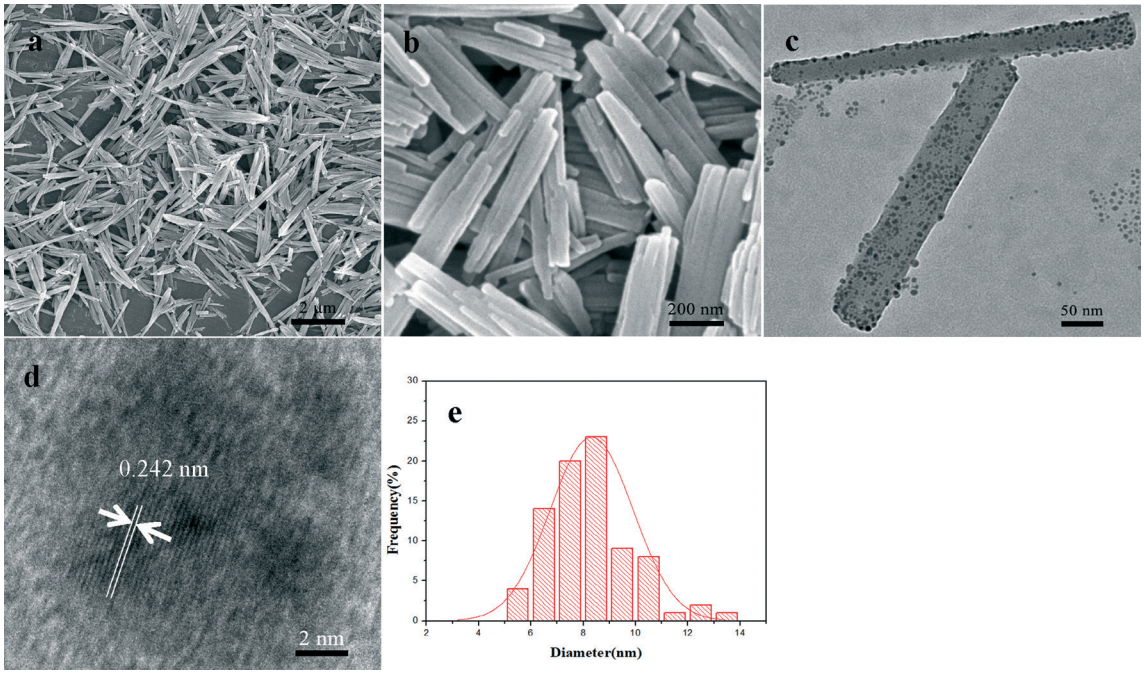

Fig. 2 SEM image (a) and magnified SEM image (b) of Ag-SD/PVA NRs; (c) TEM image of Ag-SD/PVA NRs; (d) HRTEM image of Ag-SD/PVA NRs; (e) size distribution histogram of the Ag NPs.

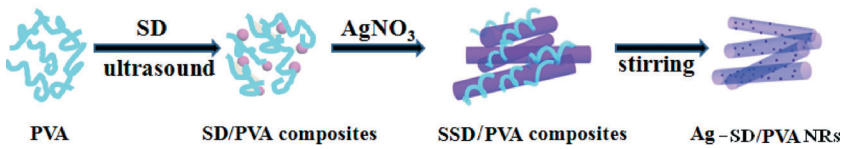

Fig. 3 Illustration of the synthetic procedure of Ag-SD/PVA NRs.

series of sample solutions with different concentrations were dispersed in sterilized tubes with 2 mL of broth media through a two-fold serial dilution method. Then, 20 μL of bacterial suspensions (10^8 CFU mL^{-1}) were added into the series of tubes. Finally, the tubes were incubated at 37 °C for 24 h and the lowest concentrations of samples that inhibited the visible growth of bacteria by the turbidimetric method were designated as the MIC values.[17] Additionally, in the MBC test, nutrient agar was spread onto a Petri plate, and then the invisible bacterial suspensions with different concentrations of samples taken out from the tubes were coated on the agar plates. The final agar plates with bacterial suspensions were incubated at 37 °C for 24 h. The number of surviving colonies was counted to get the MBC values of the samples.[2]

The antibacterial activity of the Ag-SD/PVA NRs against the tested strains was also measured by the cup diffusion method.[18] Nutrient agar was first spread onto a Petri plate, and then 100 μL of a bacterial suspension was coated on the agar plate. Subsequently, Oxford cups were placed on an agar plate, and 50 μL of the sample solution with different concentrations was added into the cup hole. Meanwhile, 0.9% sterile saline solution, which was selected as the contrast agent, was dropped into the central cups. After incubation at 37 °C for 24 h, the inhibition rings were measured to evaluate the antibacterial effect.

As shown in Table 1, the Ag-SD/PVA NRs exhibited excellent antibacterial performance compared to Ag NPs and SSD MRs, while PVA didn't exhibit antibacterial activity at all. For SSD, the MIC and MBC values of the three bacterial stains were much higher than those for Ag-SD/PVA, which was possibly attributed to the poor dissolution of SSD in the media. Additionally, the MIC values for Ag and Ag-SD/PVA were equal or nearly equal, and the MBC values for Ag were much higher than those for Ag-SD/PVA. Thus, the improved solubility of SD with small sizes and the combination of Ag with SD would contribute to the excellent antibacterial performance. Therefore, the prepared Ag-SD/PVA NRs, as new antibacterial agents, showed higher bactericidal efficacy than Ag NPs and SSD MRs.

Table 1 MIC and MBC values for PVA, Ag NPs, SSD MRs and Ag-SD/PVA NRs

	MIC (μg mL^{-1})			MBC (μg mL^{-1})		
	S. aureus	*E. coli*	*P. aeruginosa*	*S. aureus*	*E. coli*	*P. aeruginosa*
PVA	—	—	—	—	—	—
Ag	7.8	7.8	15.6	125	31.3	—
SSD	15.6	31.3	62.5	250	125	1000
Ag-SD/PVA	7.8	7.8	7.8	15.6	15.6	125

—: indicates no antibacterial properties.

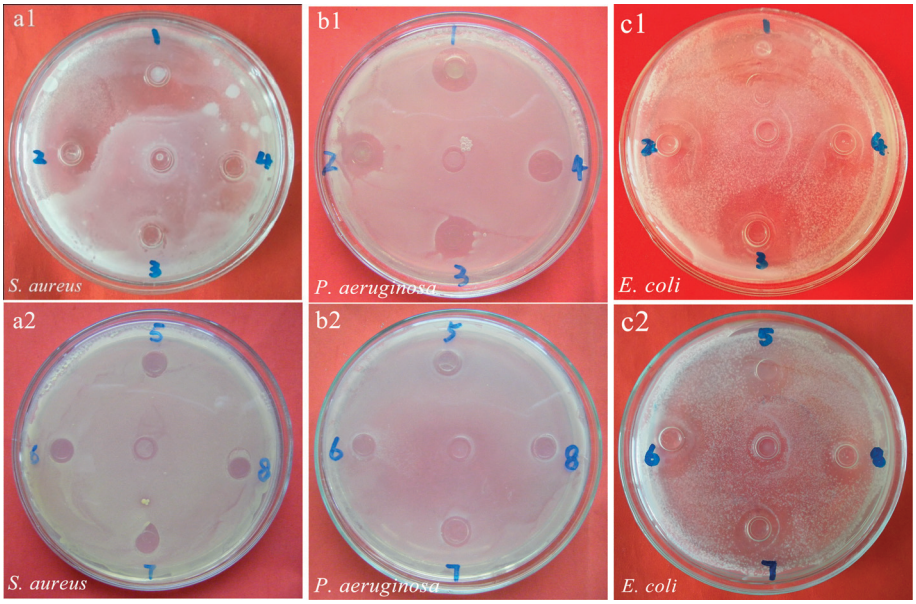

Fig. 4 Inhibition zone photographs of Ag-SD/PVA NRs against *S. aureus* (a1, a2), *P. aeruginosa* (b1, b2) and *E. coli* (c1, c2) bacteria. (1–8) Corresponding samples with concentrations of 2000, 1000, 500, 250, 125, 62.5, 31.25 and 15.62 μg mL^{-1}; the control group in the middle is 0.9% normal saline.

The antibacterial activity of Ag-SD/PVA NPs against the three strains *S. aureus*, *P. aeruginosa* and *E. coli* was further measured by the cup diffusion method (Fig. 4). Here, the concentrations of the Ag-SD/PVA sample were 2000 μg mL^{-1}, 1000 μg mL^{-1}, 500 μg mL^{-1}, 250 μg mL^{-1}, 125 μg mL^{-1}, 62.5 μg mL^{-1}, 31.25 μg mL^{-1} and 15.62 μg mL^{-1}, corresponding to the numbers from one to eight, and the control group in the middle was 0.9% normal saline. In Fig. 4a, after incubation at 37 °C for 24 h, Ag-SD/PVA hardly displayed antibacterial activity towards *S. aureus* below the concentration of 500 μg mL^{-1}. However, when the concentration was increased to 1000 μg mL^{-1} or higher, the diameter of the inhibition zones was obviously enhanced. In the case of *P. aeruginosa*, when the sample concentration was raised to 250 μg mL^{-1}, antibacterial activity was gradually displayed as the diameter of the inhibition zones increased (Fig. 4b). As shown in Fig. 4c, for *E. coli*, the diameter of the inhibition zones was always increased when the concentrations varied from low to high. Therefore, the experiments indicated that the obtained Ag-SD/PVA NRs were shown to be more sensitive towards *S. aureus* than *P. aeruginosa* and *E. coli* at higher concentrations, and more sensitive towards *E. coli* than *S. aureus* and *P. aeruginosa* at lower concentrations, which was possibly due to the synergistic antibacterial activities of the Ag NPs and SD NRs or the difference in the structure of the cell wall between Gram-negative and Gram-positive bacteria. These interesting results would be worthy to be further studied in future work.

4 Conclusions

Ag-SD/PVA NRs were successfully fabricated in an ammonia solution, with Ag NPs having a typical morphology loaded on the surface of SD/PVA NRs. The possible formation mechanism was proposed demonstrating that the SSD/PVA NR precursors were reduced by PVA to produce the Ag-SD/PVA NRs. Antibacterial activity experiments showed that the Ag-SD/PVA NRs, as new composite antibacterial agents, exhibited higher bactericidal efficacy than Ag NPs and SSD MRs alone. Furthermore, the Ag-SD/PVA NRs displayed higher antibacterial sensitivity towards *S. aureus* than *P. aeruginosa* and *E. coli* at higher concentrations, and were shown to be more sensitive towards *E. coli* than *S. aureus* and *P. aeruginosa* at lower concentrations. The reason may be the synergistic bactericidal activities of the Ag NPs and SD NRs or the difference in the structure of the cell wall between Gram-negative and Gram-positive bacteria.

Acknowledgements

Financial support to this work from the National Natural Science Foundation of China (21271062) and the Foundation of Science and Technology of Henan Province (14B150003) is acknowledged.

References

1 P. N. Kalaria, J. A. Makawana, S. P. Satasia, D. K. Raval and H. Zhu, *Med. Chem. Commun.*, 2014, **5**, 1555–1562.
2 A. Zablotskaya, I. Segal, A. Geronikaki, G. Kazachonokh, Y. Popelis, I. Shestakova, V. Nikolajeva and D. Eze, *Med. Chem. Commun.*, 2015, **6**, 1464–1470.
3 B. Li, Y. Li, Y. Wu and Y. Zhao, *Mater. Sci. Eng., C*, 2014, **35**, 205–211.
4 A. Dong, S. Lan, J. Huang, T. Wang, T. Zhao, L. Xiao, W. Wang, X. Zheng, F. Liu, G. Gao and Y. Chen, *ACS Appl. Mater. Interfaces*, 2011, **3**, 4228–4235.

5 J. R. Morones, J. L. Elechiguerra, A. Camacho, K. Holt, J. B. Kouri, J. T. Ramirez and M. J. Yacaman, *Nanotechnology*, 2005, **16**, 2346–2353.
6 N. Iqbal, M. R. A. Kadir, N. A. N. N. Malek, N. H. Mahmooda, M. R. Murali and T. Kamarul, *Mater. Lett.*, 2012, **89**, 118–122.
7 M. J. Prieto, D. Bacigalupe, O. Pardini, J. I. Amalvy, C. Venturini, M. J. Morilla and E. L. Romero, *Int. J. Pharm.*, 2006, **326**, 160–168.
8 J. Nesamony and W. Kolling, *J. Pharm. Sci.*, 2005, **94**, 1310–1320.
9 H. Kong and J. Jang, *Langmuir*, 2008, **24**, 2051–2056.
10 J. Song, H. Kong and J. Jang, *Colloids Surf., B*, 2011, **82**, 651–656.
11 M. Zasloff, *Nature*, 2002, **415**, 389–395.
12 A. Szegedi, M. Popova, K. Yoncheva, J. Makk, J. Mihaly and P. Shestakova, *J. Mater. Chem. B*, 2014, **2**, 6283–6292.
13 H. Kong, J. Song and J. Jang, *Macromol. Rapid Commun.*, 2009, **30**, 1350–1355.
14 R. Bryaskova, D. Pencheva, G. M. Kale, U. Lad and T. Kantardjiev, *J. Colloid Interface Sci.*, 2010, **349**, 77–85.
15 S. Imazato, A. Kuramoto, T. Kaneko, S. Ebisu and R. R. Russell, *Am. J. Dent.*, 2002, **15**, 356–360.
16 F. Rehman, M. Sudhaker, S. Roshan and A. Khan, *Pharmacogn. J.*, 2012, **4**, 67–70.
17 A.-T. Le, L.-T. Tam, P. D. Tam, P. T. Huy, T. Q. Huy, N. V. Hieu, A. A. Kudrinskiy and Y. A. Krutyakov, *Mater. Sci. Eng., C*, 2010, **30**, 910–916.
18 Z. Ni, Z. Wang, L. Sun, B. Li and Y. Zhao, *Mater. Sci. Eng., C*, 2014, **41**, 249–254.

